Journal of Scientific & Industrial Research
Vol. 84, August 2025, pp. 852-861
DOI: 10.56042/jsir.v84i8.11008

Exploring the Antimicrobial Potential: Synthesis, Characterization, and Insilico Study of a Ni(II) Coordination Complex with 5,7-Dibromo-8-Hydroxyquinoline

Maria Ashfaq[1]*, Noshab Qamar[1], Sameera Razi Khan[2], Ahmad Raheel[3], Hanah Nazir[1] & Wajeeha Asad[4]

[1]Department of Chemistry, University of Karachi, 75270, Karachi, Pakistan

[2]Department of Chemistry, Federal Urdu University of Arts, Science & Technology,Karachi, Pakistan

[3]Department of Chemistry, Quaid-i-Azam University, Islamabad 45320, Pakistan

[4]Department of Microbiology, University of Karachi, Karachi, Pakistan

Received 09 May 2024; revised 10 March 2025; accepted 20 June 2025

The current study involves the synthesis of the coordination complex of Ni(II) with derivatives of 8-Hydroxyquinoline in DMSO solvent in order to study their microbial properties. The physical properties of complexes such as color, solubility, melting point, molar conductivity were studied. The low value of molar conductivity shows the non-electrolytic nature of the complex. The synthesized complex was characterized quantitatively and qualitatively by using elemental analysis, FTIR spectroscopy, UV-visible spectroscopy, mass spectroscopy and powdered XRD. The spectroscopic data confirm the chelation of metal to Nitrogen and Oxygen atoms of 5,7-dibromo-8-hydroxyquinoline (HDBQ) and suggest square planar geometry of synthesized complexes. Antimicrobial activities of ligand and synthesized complex were performed against *Staphylococcus aureus*, *Pseudomonas aeruginosa*, *Salmonella typhi*, *Klebsiella pneumonia*, *Escherichia coli*, *Fusarium oxysporum*, *Rhizoctonia solani*, *Macrophomina phaseolina* and *Macrophomina* spp. Significant effects on the tested microbes is recorded. In silico studies further confirms that the complex synthesized and studied in the present work exhibit promising antibacterial activity which will contribute in the development of new antimicrobial drugs.

Keywords: Antimicrobial activity, FTIR spectroscopy, Mass spectroscopy, Metal complex, UV-visible spectroscopy

Introduction

Ligands with nitrogen and oxygen donors may result in the development of useful inorganic substances with remarkable physical characteristics.[1] The coordination chemistry of Nitrogen and Oxygen containing heterocyclic organic compounds produced from benzene, and its derivatives are of broad concern because of their miscellaneous biological behaviors, interesting spectral, magnetic, catalytic and structural properties and medical applications. They generate a large group of compounds with a wide range of therapeutic behaviors and are present in many natural products and medicines.[2] They are reported to possess a broad range of biological application, possibly due to their involvement in the donor sites of bioactive drugs.[3] Their pathogenic activity is increased on complexation with various transition and toxic metals.[4–7] Large numbers of these compounds have been manufactured and monitored for pharmacological activity.[8–10] They demonstrate a variety of different biological activities as they can behave as bactericides, fungicides, anticarcinogens, antiparasitic, antihelmintic and anti-inflammatory, anti-HIV, anti-viral, anti-diabetic, anti-cancer, anti-oxidant, anti-convulsant, anti-inflammatory, anti-proliferative, antihypertensive and analgesic. Metal ions increase the activities of these compounds on coordination.[11–14] Besides their biological significance, they form stable complexes with different transition metals.[15] Bioactive and stable metal complexes with active metal centers are useful as biological probes.[16] Significant advancement has been made in curing several diseases using transition metal complexes as drugs. Based on this development, it is crucial to investigate the biological characteristics of these complexes in order to find novel compounds with therapeutic value. Nickel plays a vital biological role as a cofactor in key enzymes, and contributes to various therapeutic applications. Nickel complexes exhibit diverse biological activities, with some serving as potential alternatives to cisplatin in cancer therapy. 8-Hydroxyquinoline, a compound based on the medicinally important quinoline

*Author for Correspondence
E-mail: maria.ashfaq@uok.edu.pk

structure, possesses a wide range of therapeutic properties. Its derivatives have demonstrated effectiveness as antimicrobials, antioxidants, anticancer, anti-inflammatory, antineurodegenerative, antimalarials, and antituberculosis agents.[11–14] Given the biological importance of nickel and its complexes, and the medicinal relevance of 8HQ derivatives, this study focuses on synthesizing and characterizing nickel(II) complexes with DBHQ ligands. Computational methods, known as in silico studies, allow researchers to investigate metal complexes virtually. This includes predicting their structure, stability, and potential biological activity, eliminating the need for initial lab experiments. A key technique within these studies is molecular docking. This method predicts how molecules, like drugs, will bind to target proteins. By simulating these interactions, docking helps determine the strength and nature of the binding, crucial for understanding biological processes and designing new drugs.

Currently, diverse bioactivities of the N and O heterocycles derivatives and their metal complexes have not been fully discovered. Keeping this in view, the current work focuses on the synthesis of new complexes containing N and O heterocyclic compounds with some metal ions. The complex will be characterized by IR and UV and mass spectroscopy. The biological properties of the complex will be examined. The investigation would be beneficial to understand the type of interactions of heavy metals with N and O heterocyclic organic derivatives having biological and industrial applications.

Experimental

Materials and Methods

Nickel Chloride ($NiCl_2$, 127.87 g/mol, purity 98%), 5,7 dibromo 8-Hydroxyquinoline ($C_9H_5Br_2NO$, 302.95 g/mol, purity 97%), DMF (C_3H_7NO, 73.09 g/mol, purity 98%), DMSO (C_2H_6OS , 78.14 g/mol, purity 98%), Sodium hydroxide (NaOH, 40 g/mol, purity 97%) and Hydrochloric acid (HCl, 36.5 g/mol, purity 97%) were purchased from Aldrich and used without further purification.

Synthesis of Complex

A solution of 4 mmol of the free ligand (5,7-dibromo-8-hydroxyquinoline, HDBQ) in 30 cm^3 DMSO was added into 4 mmol $NiCl_2.6H_2O$ in 30 cm^3 (yellow colored solution formed upon addition). The mixture was continuously stirred at ambient temperature for two hours and then the solution was kept aside until yellow precipitates formed. The complex was separated from the reaction mixture by filtration, and washed, dried and then was used for further characterization and biological assay. The percent yield of the complex was calculated.

Physical Measurements

The digital balance of Mettler model no. College 150 was used for weighing of chemicals, which have least count of ± 0.1 mg. The magnetic Stirrer of model No. 78-1 Magnetic Hot Plate was used for stirring and heating the mixture for the formation of complex. The Melting point of complex was taken on the melting point apparatus of Stuart model no. SMP10. The molar conductance of the complex was recorded on a digital direct reading conductivity meter (Jenway, 4510). UV–vis spectrum in the region of 200–800 nm and FTIR in the IR region of 400–4000 cm^{-1} of synthesized complex was recorded on UV spectrophotometer of Shimadzu model No. UV-1800 and FT-IR spectrophotometer of Shimadzu model No. IR Prestige -21 using KBr pellets. The mass spectrum of the complex was recorded on the JEOL 600H-1 spectrometer. The Costech ECS Elemental was used for the elemental analysis of the synthesized complex. Powder XRD XPERTPRO, having CuKα (λ = 1.5405 Å) as anode) was used for the characterization of the complex. The diffractogram was scanned in the range 10 to 80° with a scan speed of 6°/min. The tube voltage and tube current was adjusted to 30 mA and 40 kV, respectively.

Antimicrobial Screening

Ligand and its metal complex were tested for antibacterial potential using disc diffusion method. The refreshed bacterial cultures of *Pseudomonas aeruginosa, Staphylococcus aureus, Salmonella typhi, Klebsiella pneumonia,* and *Escherichia coli* with pre-adjusted turbidity were used to make lawns in nutrient agar plates. Absolute DMF was employed to dissolve metal complexes. Every test was performed with two replicates. The data were analyzed using analysis of variance (ANOVA) in Minitab version 15, with statistical significance set at $\boldsymbol{P} < 0.05$. Dimethyl sulfoxide (DMSO) and dimethylformamide (DMF) served as solvent controls for each dilution.

Antibacterial activities of $Ni(DBQ)_2$ were determined by agar well diffusion assay. Log phase bacterial cultures (including: *Pseudomonas*

aeruginosa, Staphylococcus aureus, Salmonella typhi, Klebsiella pneumonia and *Escherichia coli*) with a cell density of approximately 1.5×10^8 CFU/ml was spread on Muller's-Hinton Agar (MHA) petri plate with the help of cotton swab. The wells were made on inoculated MHA plate and 50 µl of sample was poured in their respective wells. MHA plates were incubated at 37°C incubator for 24 hours. Antimicrobial potential was observed by determining the zone of inhibition.

Antifungal activities of $Ni(DBQ)_2$ were determined by agar well diffusion assay. Fungal cultures inoculum was prepared by inoculating them (including: *Fusarium oxysporum, Rhizoctonia solani, Macrophomina phaseolina,* and *Macrophomina* spp.) into the Sabouraud's Dextros Broth (SDB) and incubated at room temperature for 72 hours. Fungal inoculum was spread on Sabouraud's Dextros Agar (SDA) petri plate with the help of cotton swabs. The wells were made on inoculated SDA plate and 50 µl of sample was poured in their respective wells. SDA plates were incubated at room temperature for 72 hours. Antimicrobial potential was observed by determining the zone of inhibition. Amoxyclav, Streptomycin and Gentamicin served as the positive control for comparing the efficacy of the ligand and the synthesized metal complex.

Docking Protocol

Molecular docking simulations were performed according to the reported literature[17–20] using AutoDock Vina software (version 1.1.2)[21,22] to predict the binding affinity and interactions of (DBHQ) and its Nickel metal complex with the target protein, *S. aureus* nucleoside diphosphate kinase (PDB ID: 3Q89). The Protein Data Bank was used to retrieve the "pdb" file (www.pdb.org). After the removal of all the het-atoms and the ligand, the Autodock tools were used to convert the protein to pdbqt format (1.5.6) (Morris et al. 2009).[23] The Marvin sketch (5.8.3) was used for two dimensional chemical structures of DBHQ and its Nickel complex (http://www.chemaxon.com) and these structures were then converted to 3D format by the Open Babel (ver 2.3.1).[24] Finally, "Autodock Tools" (Trott *et al*. 2010) was used to prepare the final pdbqt format of the molecules. The following parameters were used to perform the docking simulation: size x = 20; size y = 20; size z = 20; center x = 52.504760; center y = −25.474320; center z = 2.718240. The binding site on the protein was defined using the coordinates of the cytidine-5'-diphosphate binding site, which is known to interact with the *S. aureus* NDPK.[25] Twenty separate docking experiments were carried out for each compound with the docking parameters set to their default settings.

Results and Discussion

The structural characterization of the synthesized $Ni(DBQ)_2$ complex was performed by the combination of spectroscopic analysis (FT-IR, EI-MS, UV–vis), physical measurements (conductivity, solubility) and elemental analyses.

The physicochemical data of synthesized metal complexes is given in Table 1. The analytical data shows the molecular formula of the metal complex is in good agreement with the calculated elemental values of C, H, N, and metal. The yellow color complex is produced in good yield. The complex is insoluble in water, methanol and ethanol, while soluble in DMF and DMSO. Melting points were applied to portray synthesized complexes. The synthesized complex was air stable with the melting point. The molar conductance of the metal complex in DMSO (Table 1) solution falls in the range of 0.02356 $S/Cm^2/mol$. Low value of molar conductivity shows less dissociation of complex in solvents indicating that the complex behaves as non-electrolyte.[26]

Electronic Spectra

The electronic spectra furnish the details about the electronic structure of the ligand and its metal complex. The UV visible spectra of free ligands and complexes was measured in DMSO shown in

Table 1 — Physico-analytical data and elemental analysis of $Ni(DBQ)_2$ complex

Complex Mol formula	5,7-dibromohydroxyquinolinenickel(II) $[Ni(C_9H_4Br_2NO)_2]$
Molar mass g/mol	663(664.3)
Color	Yellow
Melting point (°C)	Decompose at 165°C
Yield (%)	44.40
Molar conductance ($S/Cm^2/mol$) /DMSO	0.02356
Elemental analysis (%) Calculated (Found)	
Ni	8.884 (8.86)
C	32.58 (32.63)
H	1.22 (1.22)
O	4.82 (4.83)
Br	48.20 (48.24)
N	48.20 (48.24)

Figs 1 & 2 and data is represented in Table 2. The spectra of ligand showed three ligand-centered (LC) charge-transfer peaks at 276, 354 and 406nm, which resulted from π- π* and n-π* transitions.[27–29] In complex the absorptions observed at 271, 354 and 416 nm are due to MLCT and intra-ligand transitions. While a weak absorption at 618 nm is assigned to the spin-allowed d-d transition[9,28,30–33] suggesting a square-planar nickel (II) complex.[9,33,34]

FT-IR Spectra

FT-IR spectra are the most potent techniques for detecting functional groups. The IR spectrum (Table 3) of free ligand (HDBQ) shows bands in the region of 1047.36 cm^{-1}, 3417.86 cm^{-1}, 1571.99 cm^{-1} and 1269.16 cm^{-1} which are ascribed to C-O stretching[1,13,35] O-H stretching,[36] C=N stretching (azomethine group of quinolone)[13,31,36] and C-N stretching vibrations.[36]

In Ni(DBQ]$_2$ complex shifting of bands are observed confirming the formation of complexes. The peaks appeared at 1053.13 cm^{-1}, and 1554.63 cm^{-1} are assigned to C-O stretching and C=N stretching vibrations. The C-O band in the complex underwent to a high frequency indicating formation of M-O bond.[36] The stretching vibrations of the azomethine C=N group of quinoline shifted to lower frequency suggesting that this group of heterocyclic ring is involved in the bond formation with nickel(II) ion.[13,31,36] The bands observed in the region of 450-600 cm^{-1} in complex were assigned to M-N and M-O vibrations, indicating that ligand behave as bidentate and coordinate to nickel(II) ion through N and O atom.[9,28,30–33,35,36]

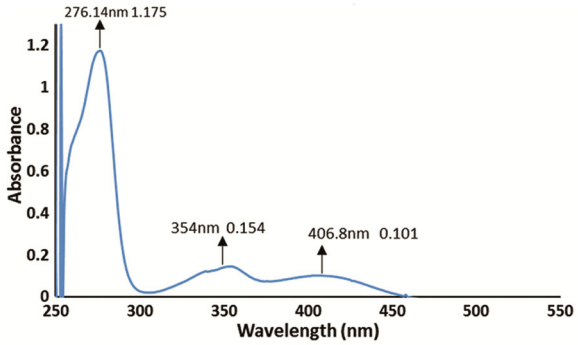

Fig. 1 — Electronic Spectra of HDBQ (10^{-5} mol/dm^3) in DMSO

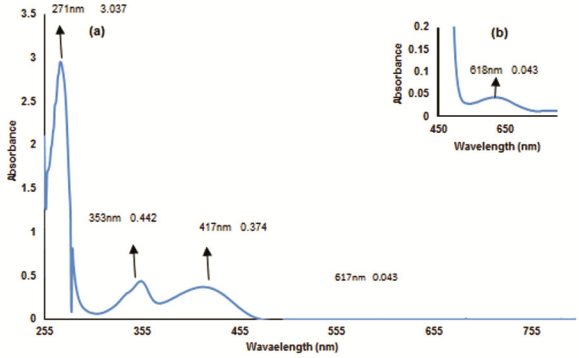

Fig. 2 — Electronic spectra of synthesized Ni(DBQ)$_2$ complex: (a) 10^{-5} mol/dm^3, (b) 10^{-3} mol/dm^3 in DMSO

Mass Spectra

The mass spectra of complex [Ni(DBQ)$_2$]$^{+2}$ showed a molecular ion peak at m/z = 664 confirming the complex formula (Scheme 1). The measured molecular mass of the complex is consistent with the expected mass and the mass spectrum of the complex (Fig. 3).

Powder X-Ray Diffraction Analysis

Powder X-ray diffraction was carried out for Ni(DBQ)$_2$ complex and spectra is presented in Fig. 4. The prominent peaks of the XRD spectrum have been indexed and examined by using a computer programme from X-pert highscore. The spectrum and related data illustrate the 2θ value, the relative intensity and interplanar distance (d-values) of each peak mentioned in Table 4. By comparing the X-ray diffraction spectra of complex with HDBQ,[37] it is clearly observed the appearance of many new peaks, which confirmed successful synthesis of NiDBQ complex. The diffraction data was used to determine the mean crystallite size (D) of the complex by Scherrer equation

Table 2 — Electronic spectral data of the HDBQ and Ni(DBQ)$_2$ complex

Compounds	Peaks (nm)	Absorbance	$\bar{\upsilon}$ (cm^{-1})	ϵ (L/mol/cm)	Assignments
HDBQ	276.4	1.175	35971	21691	π to π*
	354	0.145	28248	2677	π to π*
	406	0.101	24582	1865	n to π*
Ni(HDBQ)$_2$	271	3.037	36900	65051	LF
	354	0.442	28248	9468	LF
	416	0.374	35971	8011	MLCT
	618	0.043	16207	9.2105	d-d Transition

Table 3 — IR Spectral data of HDBQ and $Ni(DBQ)_2$ Complex

Characteristics Bands	IR frequency(cm^{-1}) HQBQ	$Ni(DBQ)_2$
(C-O)	1047.35	1053.13
OH	3417.86	
(C=N) Quinoline	1571.99	1554.63
C-N	1269.16	1300
M-N	—	584.43
M-O	—	437.84

Scheme 1 — schematic diagram for the synthesis of $Ni(DBQ)_2$ complex

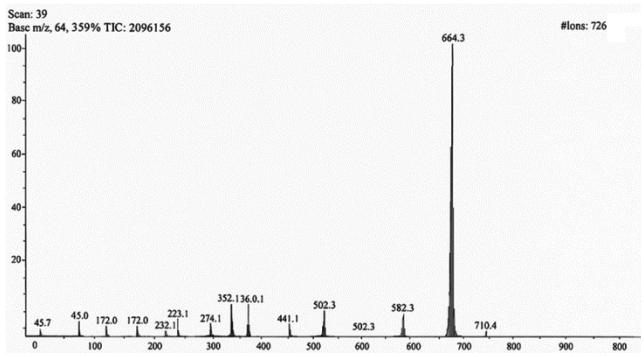

Fig. 3 — Mass spectrum of $Ni(DBQ)_2$ complex

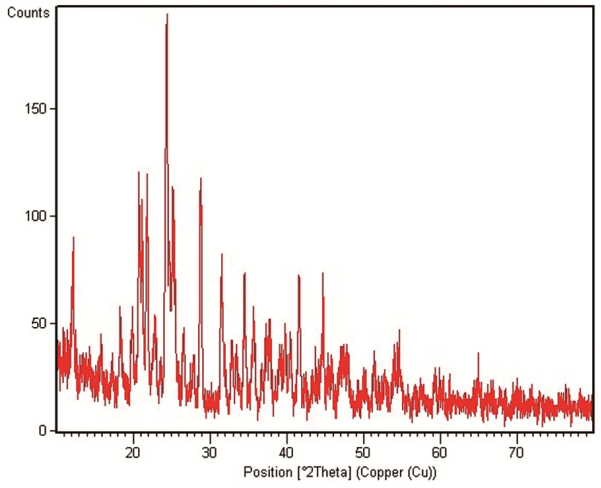

Fig. 4 — Powdered XRD spectrum of $Ni(DBQ)_2$ complex

$$D = \frac{h\,\lambda}{\beta \cos\theta} \quad \ldots (1)$$

where, h is 0.9 constant, λ is X-ray wavelength (1.5406 A°), θ is Bragg diffraction angle, and β is the full width at half maximum of the diffraction peak. The particle size was estimated by the sharp characteristic peak of the complex with the highest intensity. The crystallite size of the complex is found to be 43.1087 nm.

Table 4 — XRD data of $Ni(DBQ)_2$ complex

2θ (°)	B (°)	d-spacing (Å)	Relative Intensity (%)
12.199980	0.196800	7.25493	45.79
18.369940	0.295200	4.82976	22.95
19.933110	0.344400	4.45440	26.65
20.766130	0.246000	4.27755	55.46
21.845290	0.246000	4.06862	62.95
21.845290	0.492000	3.88985	21.34
24.287280	0.196800	3.66479	100.00
25.282220	0.295200	3.52278	51.39
26.577390	0.295200	3.35397	19.67
28.811000	0.344400	3.09884	61.36
31.478760	0.295200	2.84204	34.17
32.867980	0.295200	2.72502	16.79
34.476140	0.246000	2.60150	33.97
35.707600	0.393600	2.51456	22.38
37.878970	0.295200	2.37526	22.28
39.666480	0.787200	2.27225	13.46
41.616680	0.246000	2.17017	35.87
44.762350	0.196800	2.02470	32.92
47.537090	0.787200	1.91279	13.38
51.361270	0.295200	1.77900	10.35
54.595650	0.984000	1.68101	12.08

Antimicrobial Screening

The ligand and complex were tested as shown in Fig. 5 (a-e) against gram positive bacteria *Staphylococcus aureus* and gram negative bacteria *Pseudomonas aeruginosa*, *Salmonella typhi, Klebsiella pneumonia* and *Escherichia coli*. The zones of inhibition were measured and the following criteria were applied[12] ; low activity (1–7 mm), moderate activity (7–10 mm), high activity (11–15 mm), very high activity (≥16), and no activity (0). [41]

The zone of inhibition of synthesized complex against *Staphylococcus aureus*, *Salmonella typhi, Klebsiella pneumonia* and *Escherichia coli* bacterial strains were observed in the range of 11–15 mm which indicates its high activity as compared to *Pseudomonas aeruginosa*.

Data given in Table 5 showed that complex show better activity than the ligand towards all strains. The nickel (II) complex exhibited the highest antibacterial activity against *Klebsiella pneumoniae*. The ligand and its metal (II) complexes were evaluated for their bacterial growth inhibition efficacy in comparison to

standard antibiotics (Amoxyclav, Gentamicin, and Streptomycin). Notably, both the ligand and its metal (II) complex demonstrated inhibitory effects against *Pseudomonas aeruginosa* and *Salmonella typhi* strains resistant to Amoxyclav. Overall, the inhibition zone measurements revealed that the metal complex possessed superior bactericidal activity compared to the ligand[40] and outperformed Amoxyclav against the tested bacterial strains.

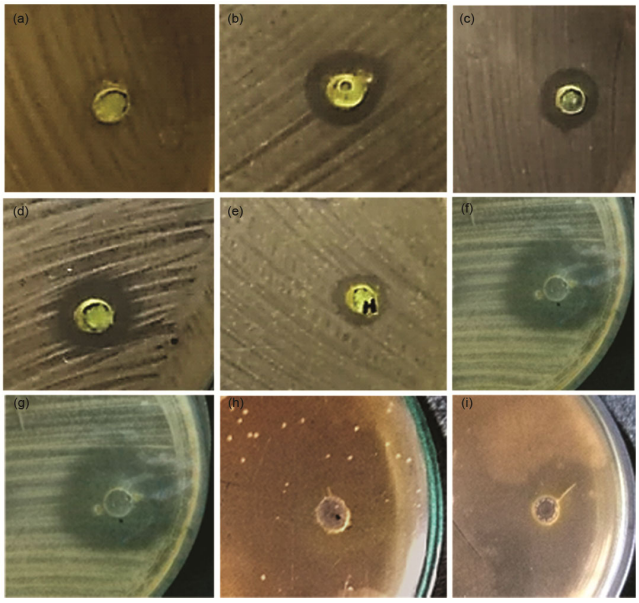

Fig. 5 — Zone of inhibition of Ni(DBQ)$_2$ complex against: (a-e) bacterial strains (a) *Pseudomonas aeruginosa*, (b) *Staphylococcus aureus*, (c) *Salmonella typhi*, (d) *Klebsiella pneumonia* (e) *Escherichia coli*; (f-i) fungal strains (f) *Fusarium oxysporum*, (g) *Rhizoctonia solani*, (h) *Macrophomina phaseolina* and (i) *Macrophomina* spp.

The examination of antifungal activity as shown in Fig. 5 (f-i) of ligand, its metal complex against antifungal pathogens, including *Fusarium oxysporum, Rhizoctonia solani, Macrophomina phaseolina, Macrophomina* spp. revealed that the complex show pronounced antifungal activity (Table 5). The zone of inhibition of synthesized complex against *Fusarium oxysporum, Rhizoctonia solani, Macrophomina* spp. fungal strains were observed in range of ≥16 mm which indicates its very high activity while complex also has significant activity against *Macrophomina phaseolin.*

The highest activity of complex was observed against *Macrophomina* spp. The metal complex is observed to be the better antifungal agent against all strains as compared to ligand and standard drug (Carbendazim).

The increase in biocidal activity can be explained on the basis of chelation theory. Studies indicate that structural motifs containing an additional (C=N) bond with nitrogen and oxygen donor systems can inhibit enzyme activity by deactivating them through metal coordination. Furthermore, ligands with such donor

Table 5 — Antimicrobial screening data of HDBQ, Ni(DBQ)$_2$Complex and standards

	Zone of inhibition (mm)) against bacterial strain				
	Pseudomonas aeruginosa	*Staphylococcus aureus*	*Salmonella typhi*	*Klebsiella pneumonia*	*Escherichia coli*
HDBQ	4 ± 5.657	12 ± 0.000	11 ± 4.243	12 ± 2.828	11 ± 1.414
Ni(DBQ)$_2$	6 ± 8.485	14 ± 0.000	14 ± 2.828	15 ± 1.414	11 ± 1.414
DMSO	—	—	—	—	—
DMF	—	—	—	—	5 ± 7.071
Amoxyclav[41]	—		—		8
Gentamicin[41]	14		10.5		9
Streptomycin[42] (20 µg/disc)		10	8		9

	Zone of inhibition (mm)against fungal strain			
	Fusarium oxysporum	*Rhizoctonia solani*	*Macrophomina phaseolina*	*Macrophomina* spp.
HDBQ	10 ± 0.000	08 ± 0.000	09 ± 0.000	10 ± 0.000
Ni(DBQ)$_2$	18 ± 0.000	16 ± 0.000	12 ± 0.000	20 ± 0.000
DMSO	—	—	—	—
DMF	—	—	—	—
Carbendazim[42] (20 µg/disc)	9	7	10	

(-)* As expected no zone of inhibition was observed for DMSO and DMF; The values are the arithmetic mean of the zone of inhibition ± standard deviation

systems may suppress enzyme production, as enzymes dependent on these functional groups for activity are particularly vulnerable to metal-ion-induced deactivation upon chelation. Chelation of metal causes reduction in the polarity of metal ions by sharing its partial charge with the donor atom of ligand. Furthermore, it enhances the delocalization of π-electrons across the entire chelate ring, thereby increasing the complex's lipophilicity. This improved lipophilicity facilitates stronger interactions with the lipid membrane and blocks metal-binding sites in bacterial enzymes. According to Overton's concept of cell permeability, the lipid bilayer selectively permits the passage of lipid-soluble compounds. Thus, lipophilicity serves as a critical determinant of bactericidal efficacy**.** Heterocyclic ligand (free or complexes with metal) possessing multifunctional groups will be able to interact with nucleic bases or metal ions present in living systems. Thus complexation can be adopted to control biological growth. This supports that complex can behave as active biocidal agent.[38–40]

A solvent control test was performed, adding DMSO and DMF to the test medium using the same protocol as the main experiment, to confirm their neutrality on bacterial growth. The antibacterial activities were calculated as mean ± SD of three replicates.

Docking Study

The capacity of *Staphylococcus aureus*, a versatile human pathogen, to cause a wide range of infections, including skin and soft tissue infections, pneumonia, and serious bloodstream infections, makes it a substantial public health problem. Targeting important enzymes inside the bacterium's metabolic pathways is a viable technique in the context of antibacterial medication development. One such enzyme, *S. aureus* nucleoside diphosphate kinase (NDK), is a major role in nucleotide metabolism, which is required for bacterial reproduction and survival. The transfer of phosphate groups between different nucleoside diphosphates is catalyzed by NDK, which affects the cellular pool of nucleotide triphosphates necessary for DNA and RNA synthesis. As a result, reducing NDK activity in *S. aureus* can disrupt important cellular processes, making it a promising target for the development of new antibacterial medicines. Furthermore, the emergence of drug-resistant strains of *S. aureus* highlights the critical need for novel treatment techniques, stressing the necessity of investigating targets such as *S. aureus* NDK in the search for effective antibacterial medicines. Because this enzyme is restricted to bacteria and differentiates greatly from its human equivalent, medicines that precisely block the bacterial enzyme without impacting human nucleoside diphosphate kinase might be developed. This selectivity in possible antibacterial medicines might result in lower toxicity and fewer adverse effects.

With binding energies of −6.1 and −6.2 kcal/mol, respectively (Table 6), the outcomes of the molecular docking simulations demonstrated that DBHQ and its metal complex exhibited strong binding affinities for *S. aureus* nucleoside diphosphate kinase. The metal complex exhibited marginally higher binding affinity than the free ligand (DBHQ), indicating that coordination of the metal ion to the ligand enhanced the ligand's binding to the protein.

Both ligand and complex interacted with the *S. aureus* nucleoside diphosphate kinase through multiple interactions (Hydrogen bonds, Electrostatic, hydrophobic and Van der Waals) with critical amino residues in the active site, as determined by analyzing the binding modes of DBHQ and its metal complex. The hydroxyl group and Nitrogen of DBHQ specifically created hydrogen bonds with the side chains of Lys9 and Asn112, whereas the bromine atoms formed halogen interactions with His52 and Phe57, while pi-sigma interactions were also observed with Thr91 (Fig. 6 a & b). In contrast, the metal complex formed Pi-cation with the Mg ion, Pi-anion with Asp118, Pi-Pi stacked with His52, Pi-alkyl with Tyr49, His52 and His115, Alkyl interaction with Leu61 and Van Der Waal interaction with, Lys9, Glu51, Lys55, Phe57, Thr91, Arg102, Gly116 (Fig. 9 and 10).

In conclusion, the results imply that both DBHQ and its metal complex have the potential to inhibit the activity of *S. aureus* nucleoside diphosphate kinase, a key enzyme in nucleotide metabolism that has been identified as a potential target for the development of antibacterial drugs.[43–44] To validate these results and assess the antibacterial activity of these compounds, additional experimental research is required.

Table 6 — Binding energies of $Ni(DBQ)_2$Complex with *S. aureus nucleoside diphosphate kinase*

Compound	Binding affinity (kcal/mol)
HDBQ	−6.1
$Ni(DBQ)_2$	−6.2

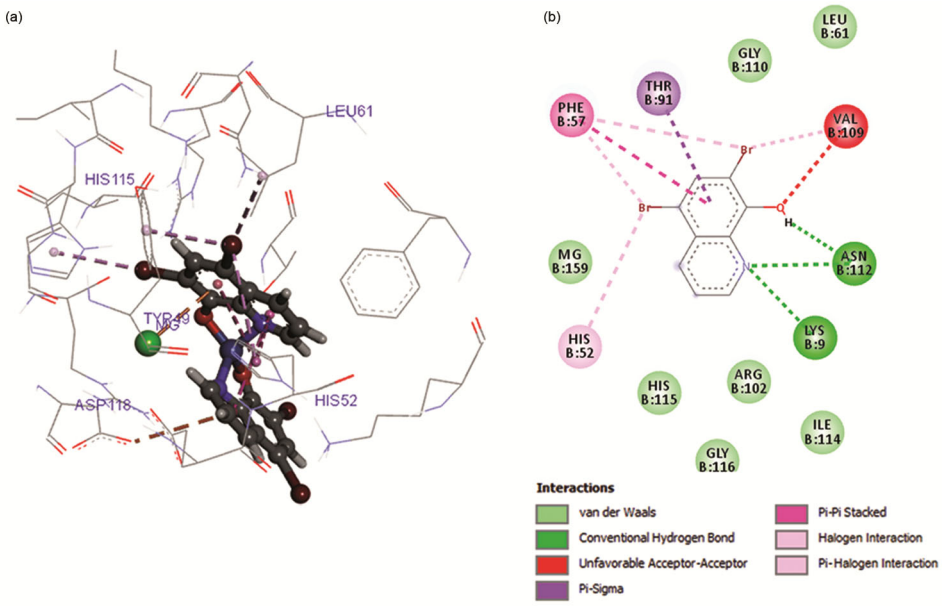

Fig. 6 — Docking of **(1)** in active site *S. aureus* nucleoside diphosphate kinase: (a) 3D depictions (b) 2D depictions

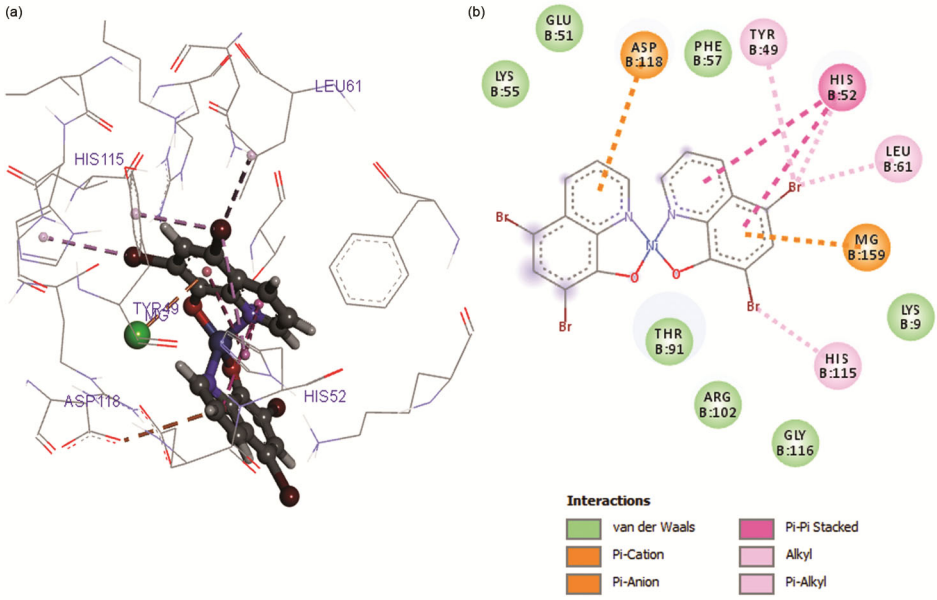

Fig. 7 — Docking of **(2)** in active site *S. aureus* nucleoside diphosphate kinase: (a) 3D depictions, (b) 2D depictions

Conclusions

The synthesized complex was characterized by IR spectra, electronic spectra, mass spectra, powdered XRD and molar conductance. The obtained results concluded that nickel forms a square planar complex with DBHQ. Low value of molar conductivity indicating the complex behaves as non-electrolyte. Molecular docking analysis was carried out for confirming the experimental observations. The synthesized complex exhibits higher antimicrobial activity than ligand due to chelation. Since good antifungal activity have been observed for the synthesized complex, the further study of biological activity of the complex will be carried out in more detail in future. A broader understanding of the complex's activity against different pathogens will improve its potential for clinical applications, which in turn will facilitate the development of new treatments for a wider range of infectious diseases. Thus, there is hope that the studied complex could reasonably be used in designing more potent antibacterial agents for the treatment of some

common diseases. To overcome the challenge of poor aqueous solubility various strategies are employed, including surfactant addition, cosolvency, complexation and pH alteration. Among them, the most effective method of cosolvency will be used in future to solubilize metal complexes so that it can be used for wide applications.

References

1 Patel K B, Kharadi G J, Vyas K B & Nimavat K S, The Metal Complexes of [5-(n-Butoxymethyl-8-Quinolinol) and 8-quinolinols] mixed. Ligand: A new transition metal complexes with In-vitro antifungal activity, *Int J Pharm Res Scholars*, **1** (2012) 474–480.

2 Durosinmi L M, Oluduro A O & Oseni M, Synthesis, characterization and antimicrobial properties of benzimidazole derivatives and their metal complexes, *J Appl Chem,* **10** (2017) 24−45.

3 Sarkar K, Sen K, Some drugs in action: metal ions do influence the activity, *Int J Pharm Sci Res,* **6** (2015)1−13, http://dx.doi.org/10.13040/IJPSR.0975-8232.6(1), 1–13

4 Rajeshirke M, Shah R, Yadav P & Purohit NV, Synthesis and antioxidant activity of Metal (II) complexes of isocoumarin derivatives, *Der Pharmacia Sinica*, **3** (2012) 239–248.

5 Ad-Daraji I I S & Al Samarrai A S H, synthesis of quinoline derivatives by reaction of dimethyl(2R,3S,4R)-2-Phenyl-4-(Phenylamino)-1,3,4-Trihydroquinoline-2,3-dicarboxylate with some amines, *Int J Pharm Sci Res*,**7** (2016) 961-967, DOI:10.13040/IJPSR.0975–8232.

6 Asif M, A Mini Review: biological significances of nitrogen heteroatom containing heterocyclic compounds, *Int J Bioorg Chem,* **2** (2017) 146-152, DOI: 10.11648/j.ijbc.20170203.20.

7 Selvaganapathy M & Raman N, Pharmacological activity of a few transition metal complexes: a short review, *J Chem Biol Ther,* 1 (2016) 17, DOI: 10.4172/2572-0406.1000108.

8 Sgarlata C, Arena G, Bonomo RP, Giuffrida A & Tabbì G, Simple and mixed complexes of copper(II) with 8-hydroxyquinoline derivatives and amino acids: Characterization in solution and potential biological implications, *J Inorg Biochem*, **180** (2018) 89–100, DOI: 10.1016/j.jinorgbio.2017.12.002.

9 Yin X, Ma K, Wang Y, Sun Y, Shang X, Zhao Z, Wang R, Chen Y, Zhu J & Liu Y, Design, synthesis, and antifungal evaluation of 8-Hydroxyquinoline metal complexes against phytopathogenic fungi, *J Agric Food Chem*, **68** (2020) 11096–11104, https://doi.org/10.1021/acs.jafc.0c01322.

10 Witwit I N, Motaweq Z Y & Mubark H M, Synthesis, characterization, and biological efficacy on new mixed ligand complexes based from azo dye of 8-hydroxy quinoline as a primary ligand and imidazole as a secondary ligand with some of transition metal ions, *J Pharm Sci Res,***10** (2018) 3074–3083.

11 Litecká M, Samoľová E, Obuch J, Kubíček V, Vilková M, Kepeňová M & Potočňák I, Synthesis, solution stability, and structural characterization of quinolinol-based silver(I) complexes, *J Coord Chem*, 73 (2020) 784–795, DOI: 10.1080/00958972.2020.1758681.

12 Meng T, Qin Q, Zou H, Wang K & Liang F, Eighteen 5, 7-Dihalo-8-quinolinol and 2,2′-Bipyridine Co(II) complexes as a new class of promising anticancer agents, *ACS Med Chem Lett,* **10** (2019) 1603–1608, https://doi.org/10.1021/acsmedchemlett.9b00356.

13 Elsherif K M, Aberrwaila H, Aburowais A S, Etwaish A M & Elassawi A M, Complexation of Ag(I) with 8-Hydroxyquinoline: Synthesis, spectral studies and antibacterial activities, *Adv J Chem Sec A,* **5** (2022) 138–146, https://doi.org/10.22034/ajca.2022.322123.1294.

14 Guerreiro C T R, Ribeiro C A & Crespi M S, Study of the alkaline earth metals with 8-hydroxyquinolinate derivatives, *J Therm Anal Calorim,* **70** (2002) 437–445.

15 Hussain T, Pakistan at the verge of potential epidemics by multi-drug resistant pathogenic bacteria, *Adv Life Sci,* **2** (2015) 46–47.

16 Dhanaraj C J, Hassan I, Johnson J, Joseph J & Joseyphus R S, Synthesis, spectral characterization, DNA interaction, anticancer and molecular docking studies on some transition metal complexes with bidentate ligand, *J Photochem Photobiol B Bio,* **162** (2016) 115–124, DOI: 10.1016/j.jphotobiol.2016.06.032.

17 Raheel A, Imtiaz-ud-Din, Hassan I S, Babar T M, Rabia A, Zafar A, Abbas S & Mundher A.-S, Synthesis, antimicrobial activity, urease inhibition and molecular docking studies of new proline linked thiourea derivatives, *Rev Roum Chim*, **65** (2020) 783–788, DOI:10.33224/rrch.2020.65.9.03.

18 Raheel A, Imtiaz-ud-Din, Taj M B, Tahir M N & Al-Shakban M, Synthesis, structures, and molecular docking of some bioactive benzamide derivatives as ionic solids, *Russ J Gen Chem*, **88** (2018) 1508–1514.

19 Qamar N, Sultan H, Raheel A, Ashfaq M, Azmat R, Naz R, Lateef M, Khan K M & Arshad T, Heterochelates of metals as an effective anti-Urease agents couple with their docking studies, *Pak J Pharm Sci*, **32** (2019) 1179–1183.

20 Hameed K, Rubina S, Raheel A, Taj B, Iftkhar SH, Imtiaz-ud-Din, Sadiqa A & Aslam A, Design, synthesis, docking and in vitro antibacterial study of fluoro substituted schiff bases, *J Chem Soc Pak*, **40** (2002) 782–791.

21 Eberhardt J, Santos-Martins D, Tillack AF & Forli S, AutoDock Vina 1.2.0: New docking methods, expanded force field, and python bindings, *J Chem Inf Model,* **61** (2021) 3891–3898, https://doi.org/10.1021/acs.jcim.1c00203.

22 Trott O & Olson A J, AutoDock Vina: improving the speed and accuracy of docking with a new scoring function, efficient optimization, and multithreading, *J Comput Chem*, **31** (2010) 455–461, DOI: 10.1002/jcc.21334.

23 Morris G M, Huey R, Lindstrom W, Sanner M F, Belew R K, Goodsell D S & Olson A J, AutoDock4 and AutoDockTools4: Automated docking with selective receptor flexibility, *J Comput Chem*, **30** (2009) 2785–2791, DOI: 10.1002/jcc.21256.

24 O'Boyle N M, Banck M, James C A, Morley C, Vandermeersch T & Hutchison G R Open babel: An open chemical toolbox, *J Cheminform*, **3** (2011) 33, DOI: 10.1186/1758-2946-3-33.

25 Srivastava S K, Rajasree K & Gopal B, Conformational basis for substrate recognition and regulation of catalytic activity in Staphylococcus aureus nucleoside di-phosphate kinase, *Biochim Biophys Acta,* **1814** (2011) 1349–1357, DOI: 10.1016/j.bbapap.2011.06.008.

26 Wankhede D S, Kulkarni P A, Jadhav N S, Gurle M D, Wagh P B & Shankarrao O, Synthesis and characterization of

biologically active mixed ligand complexes of 8-Hydroxyquinoline and Salicylaldehyde, *Asian J Res Chem*, **6** (2013) 525–530.

27 Yadav B S, Singhal S & Chand S, Electronic absorption spectra of 5,7-Dibromo-8-hydroxy Quinoline, *Asian J Chem*, **20** (2008) 925–928.

28 Abdulsalam M B & Numan A T, Characterization, and biological activity of mixed ligand complexes from 8-Hydroxyquinoline and new Ligand for β-Enaminone, *Pak J Med Health Sci*, **16** (2022) 614–621. DOI: https://doi.org/ 10.53350/pjmhs221686

29 Obaid S M H, Jarad A J & Al-Hamdani A A S, Synthesis, characterization and biological activity ofmixed ligand metal salts complexes with various ligands, *J Phys Conf Ser,* **1660** (2020) 012028, DOI: 10.1088/1742-6596/1660/1/012028

30 Witwit I N, Motaweq Z Y & Mubark H M, Synthesis , characterization, and biological efficacy on new mixed ligand complexes based from azo dye of 8-hydroxy quinoline as a primary ligand and imidazole as a secondary ligand with some of transition metal ions, *J Pharm Sci Res*, **11** (2019) 508–518.

31 Muthukumar C, Sabastiyan A, Valarselvan S, Subramanian M & Shanmugavadivel M, synthesis, characterization and antimicrobial activity of manganese(II) and nickel(II) complexes of 7-diethylaminobenzyl-8-hydroxyquinoline, *J Adv Chem*, **12** (2016) 4324–4332, DOI: 10.24297/JAC.V12I4.2172

32 Abuthahir S S S, Nasser A J A, Rajendran S & Brindha G, Synthesis, spectral studies and antibacterial activities of 8-Hydroxyquinoline derivative and its metal complexes, *Chem Sci Trans,* **3** (2014) 303–313. DOI:10.7598/cst2014.641

33 Zhang Q L & Zhu B X Square-planar nickel(II) complexes with a tridentate Schiff base and monodentate heterocycles: self-assembly to dimeric and one-dimensional array via hydrogen bonding, *J Coord Chem*, **61** (2008) 2340–2346, DOI:10.1080/00958970801914074

34 Sujamol M S, Athira C J, Sindhu Y & Mohanan K, Synthesis, spectroscopic characterization, electrochemical behaviour and thermal decomposition studies of some transition metal complexes with an azo derivative, *Spectrochim Acta A Mol Biomol Spectrosc*,**75** (2010) 106–112, https://doi.org/10.1016/j.saa.2009.09.050

35 Patel K D & Patel H S, Synthesis, spectroscopic characterization and thermal studies of some divalent transition metal complexes of 8-hydroxyquinoline, *Arab J Chem*, **10** (2017) S1328–S1335. https://doi.org/10.1016/j.arabjc.2013.03.019

36 Lakshmi P A, Balachandran V & Janaki A Comparative vibrational spectroscopic studies, HOMO–LUMO and NBO analysis of 5,7-dibromo-8-hydroxyquinoline and 5,7-dichloro-8-hydroxyquinoline based on density functional theory, *J Mol Struc,* **1004** (2011) 51–66, https://doi.org/10.1016/j.molstruc.2011.07.022

37 Zhu C, Farajtabar A, Wu J & Zhao H, 5,7-Dibromo-8-hydroxyquinoline dissolved in binary aqueous co-solvent mixtures of isopropanol, N,N-dimethylformamide, 1,4-dioxane and N-methyl-2-pyrrolidone: Solubility modeling, solvent effect and preferential solvation, *J Chem Thermodyn*, **148** (2020) 106138, https://doi.org/10.1016/j.jct.2020.106138

38 Vashi R T, Patel S B & Kadiya H K, Synthesis, characterization and antimicrobial activity of metal Chelates of 2-[(8-hydroxyquinolinyl)-5-aminomethyl]-3-(4-Bromophenyl)-3(H)- quinazolin-4-one, *Der Pharma Chem*, **4** (2012) 1506–1511.

39 Jyotirmaya S, Nandini S P K & Kumar P S, In vitro Antimicrobial investigations of newly synthesized transitional bivalent metal complexes derived from 8-Hydroxyquinoline, *Ind J Pharm Edu Res* **51** (2017) 480–489, DOI:10.5530/ijper.51.3.76.

40 Patel K B, Kharadi G J & Nimavat K S, Synthesis and description of transition metal complexes and antimicrobial studies, *J Chem Pharm Res*, **4** (2012) 2422–2428.

41 Ommenya F K , Nyawade E A, Andala D M & Kinyua J, Synthesis, Characterization and Antibacterial activity of schiff base, 4-Chloro-2-{(E)-[(4-Fluorophenyl)imino] methyl}phenol metal (II) complexes, *J Chem* (2020) 1–8. https://doi.org/10.1155/2020/1745236.

42 Korejob F, Noreen R, Ali S A, Humayun F, Rahman A,Sultana V & Ehteshamul-Haque, Evaluation of antibacterial and antifungal potential of endophytic fluorescent pseudomonas associated with salvadora persica L. and salvadora oleoides decne*, Pak J Bot*, **49(5)** (2017) 1995–2004.

43 Nabil M, Adly O M, Shebl M, Taha A & Samy F, Ni II and Co II binary and ternary complexes of 3-formylchromone: spectroscopic characterization, antimicrobial activities, docking and modeling studies, *RSC Adv*, **12** (2022) 29939–29958, DOI: https://doi.org/10.1039/D2RA03475A.

44 Pahonțu E, Proks M, Shova S, Lupaşcu G, Ilieş D C, Bărbuceanu S F, Socea L I, Badea M, Păunescu V, Istrati V D, Gulea A, Drăgănescu D & Pîrvu C E D, Synthesis, characterization, molecular docking studies and in vitro screening of new metal complexes with Schiff base as antimicrobial and antiproliferative agents, *Appl Organomet Chem*, **33** (2019) e5185. https://doi.org/10.1002/aoc.5185.